Direct Tissue Analysis by Matrix-Assisted Laser Desorption Ionization Mass Spectrometry: Application to Kidney Biology

Kristen D. Herring,* Stacey R. Oppenheimer, PhD,* and Richard M. Caprioli, PhD[†]

Summary: Direct tissue analysis using matrix-assisted laser desorption ionization mass spectrometry (MALDI MS) provides in situ molecular analysis of a wide variety of biological molecules including xenobiotics. This technology allows measurement of these species in their native biological environment without the use of target-specific reagents such as antibodies. It can be used to profile discrete cellular regions and obtain region-specific images, providing information on the relative abundance and spatial distribution of proteins, peptides, lipids, and drugs. In this article, we report the sample preparation, MS data acquisition and analysis, and protein identification methodologies used in our laboratory for profiling/imaging MS and how this has been applied to kidney disease and toxicity.
Semin Nephrol 27:597-608 © 2007 Elsevier Inc. All rights reserved.
Keywords: *MALDI, direct-tissue analysis, imaging mass spectrometry, LCM, drug-toxicity, renal cancer*

Matrix-assisted laser desorption ionization mass spectrometry (MALDI MS), introduced in the late 1980s,[1,2] has become an enabling analytic technology to study proteins in biological systems because of its molecular specificity and high-throughput capabilities.[3,4] One of the more recent developments to this technology is its application to direct tissue analysis for both molecular profiling and imaging.[5] The technology allows for the analysis of molecules in tissues without the need for target-specific reagents such as antibodies or the need for tissue homogenization, thereby maintaining the integrity of the tissue sample and allowing assessment of molecular spatial distribution.

The principles of MALDI MS have been described.[2,6-9] In brief, the analyte of interest is mixed with an energy-absorbing compound (matrix) on a MALDI target plate. As the solvent evaporates, the analyte co-crystallizes with the matrix. Inside the mass spectrometer, molecules are desorbed from the sample by irradiation with an ultraviolet laser. In this process, analytes become protonated and primarily give rise to $[M+H]^+$ ions that subsequently are measured according to their mass-to-charge ratio (m/z). Typically, the time-of-flight (TOF) analyzers are used to measure m/z values of ions (Fig. 1).[8,9]

MALDI MS can be used to profile molecules in a sample (ie, analyze a small number of discrete spots scattered throughout the sample), or image a sample (ie, systematically raster across a tissue section to produce an ordered array of spots). In the latter, the laser performs a raster over the tissue surface in a predefined 2-dimensional array or grid, generating a full mass spectrum at each grid coordinate. Mass spectra acquired in this manner display ions in the m/z range of 500 to more than 100,000, corresponding to many hundreds of different
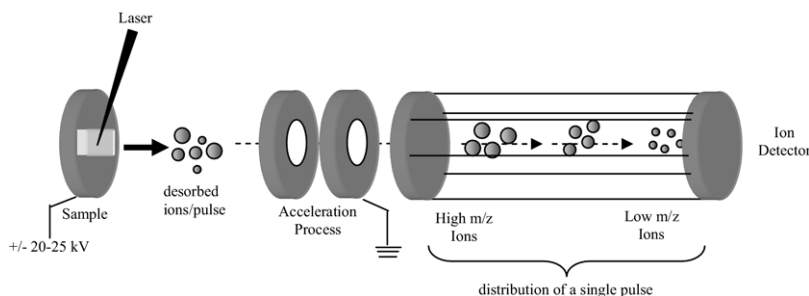
Figure 1. MALDI-TOF. A sample is irradiated with a brief laser pulse and molecules are desorbed from the surface. Energy is absorbed by the matrix and transferred to the analyte, which becomes protonated and then is accelerated down a field-free drift tube. Ions collide with a detector at the end of this tube and their TOF is measured and through calibration converted to m/z.

molecules present in the tissue. The coordinates of the irradiated spots are used to generate 2-dimensional ion density maps, or images, that represent individual m/z values with their corresponding intensities (Fig. 2). Likewise, drug analysis in tissue can be accomplished by monitoring the protonated drug or its metabo-

lites and their corresponding fragments at each discrete coordinate of such an array.

Direct tissue analysis by MALDI has been used to detect drugs and their metabolites[10-13] as well as intact proteins and peptides[14,15] directly from tissue. Profiling/imaging MS has been used to study molecular aspects of cancer, providing
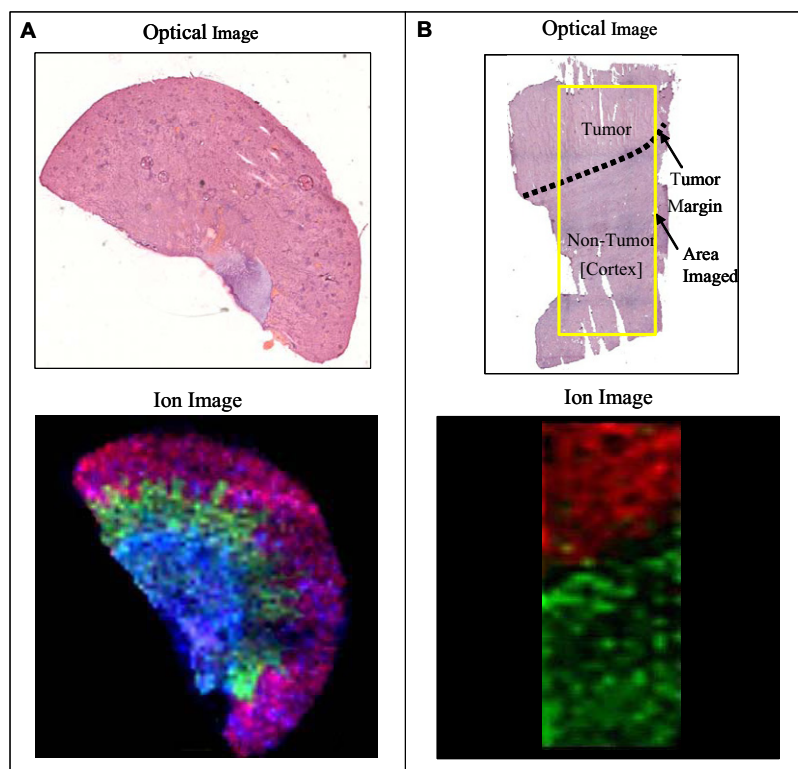

Figure 2. Images generated by imaging MALDI MS. (A) Optical hematoxylin-eosin stained (top) and overlaid ion images (bottom) of a normal rat kidney section. Shown are 3 ions represented in color to indicate localization (pink: m/z 8,451 in the cortex, green: m/z 8,560 in the outer medulla, blue: m/z 4,965 localized primarily in the inner medulla). (B) Optical hematoxylin-eosin stained (top) and ion images (bottom) of a human ccRCC tissue section with tumor and adjacent nontumor tissue. Shown are 2 overlaid ions (red: m/z 11,090 localized to tumor, green: m/z 4,563 in nontumor cortex).

tumor-specific markers as well as diagnostic- and prognostic-specific markers.[16,17] In this article, we describe the current profiling/imaging methodologies used in our laboratory and their application to glomerulosclerosis, drug-induced renal toxicity, and renal cancer.

SAMPLE PREPARATION FOR PROFILING AND IMAGING TISSUES BY MS

Direct MS analysis usually is performed on tissues that have been excised and immediately frozen in liquid nitrogen to maintain tissue morphology and to minimize molecular degradation. Maintaining the integrity of the tissue throughout this process maximizes the information obtained in the analyses by ensuring that the original 3-dimensional structure is not compromised and the molecular species monitored have not been altered as a result of the sample procurement and preparation process.

Frozen tissues are sectioned in a cryostat, if necessary, using a small amount of optimum cutting temperature media on the cutting block for support. Preferably, tissue should not be embedded in the polymer media because surface contamination with polymer caused by the cutting process tends to reduce ionization efficiency. A cryostat temperature between $-15°C$ and $-25°C$ generally is optimal for sectioning kidney tissue. Sections generally are cut at 12 μm thickness, but may range between 10 and 20 μm depending on the application.[4,10] After cutting, sections are thaw-mounted onto a MALDI target plate and washed and/or allowed to dry in a vacuum desiccator.

It is advantageous to wash tissue sections that are rich in salts and other contaminants as well as hemoglobin before matrix deposition because these species can contribute to a high spectral baseline and generalized signal suppression. Because of the kidney's role in filtration of blood, washing kidney sections removes excess hemoglobin and salts and enhances signal quality. The conventional tissue washing method involves 2 separate 70% ethanol submersions for 20 to 30 seconds followed by 10 to 15 seconds in 95% 200-proof ethanol (or 100% reagent grade ethanol). Ethanol is a known tissue fixative in histology[18] and delocalization of

proteins appears not to be significant; however, it is noted that proteins soluble in these aqueous solutions may be removed during the washing step. Previous studies have indicated minimal protein loss during this process, but the washing procedure should be confirmed for each tissue type.[19,20]

Selection of the matrix/solvent combination for direct tissue analysis depends on the molecular weight, hydrophobicity, and salt content of the analyte. Typically, 3,5-dimethoxy-4-hydroxycinnamic acid (sinapinic acid) is favorable for proteins (molecular weight > 2 kDa), and α-cyano-4-hydroxycinnamic acid (CHCA) is optimal for peptides (500-2,000 Da). Small-molecule analysis, including drugs and lipids, usually is performed with 2,5-dihydroxybenzoic acid. The optimal matrix concentration range is 10 to 30 mg/mL sinapinic acid for protein analysis and 10 to 20 mg/mL CHCA for peptide analysis. The usual matrix solvent is 50% acetonitrile with 0.1% trifluoroacetic acid (TFA). More nonpolar solvents such as methanol or isopropanol can be used for more hydrophobic molecules. The optimal matrix/solvent combination may vary between tissue types and analytes and must be assessed for each study.

Various methods of matrix deposition on thin tissue sections have been used successfully. For tissue profiling, matrix can be deposited manually either with a pipette or pulled glass capillary. Syringe pumps provide an alternative, more automated approach with higher reproducibility and smaller matrix spot diameters. Robotic deposition offers superior reproducibility, smaller matrix spot diameters, and a higher throughput platform, and also allows for the ability to perform histology-directed analyses[21] and imaging. Two types of robotic devices, an acoustic spotter[19] and a chemical inkjet printer,[22] have been used successfully for tissue profiling and imaging. General matrix deposition guidelines for both robotic types have been described,[19,22] but for each tissue type, method optimization is recommended to determine the number of matrix drops and passes required to obtain high-quality spectra. In some cases matrix seeding may be desired to aid in the crystallization process.[19] The current minimum spot-to-spot spacing achievable with

commercial robotic spotters is in the range of 100 to 200 μm. For applications that require a resolution higher than 100 μm, spray coating may be used. A spray coating device may be as simple as a glass thin layer chromatography spray nebulizer that generates and sprays fine droplets of matrix under slight positive pressure, or automated spray devices. The matrix solution must wet the tissue surface to ensure co-crystal formation between matrix and analyte. For manual spraying methods, a 1-minute delay between passes provides sufficient drying time. Multiple passes are necessary to coat the entire tissue, but overcoating can suppress analyte signal. The matrix coverage can be monitored as necessary under a microscope.

Histology-Directed MS Analysis

Region specificity is important for analysis of heterogeneous tissue types such as kidney. One MALDI-compatible method to accomplish this is to stain tissues using cresyl violet stain or other suitable stains (H&E stains give poor MS results), allowing histology and MS analysis to be performed on the same tissue section with minimal interference in signal quality.[23] This method usually requires that tissue sections be applied to a conductive glass slide to obtain histopathologic detail. A new method, histology-directed MS analysis, uses digital imaging to merge traditional histopathology, or hematoxylin-eosin tissue staining, with tissue profiling (Fig. 3). Details of this methodology have been reported.[21] In brief, a pathologist systematically can select areas on a stained tissue section with the usual cellular specificity. By co-registration, the spot coordinates are transferred to a robotic matrix spotter and then to the mass spectrometer. This allows the profiles and other data-processing algorithms such as statistical analysis to be mapped directly onto the histologic image and correlation between molecular profiles and histopathology.

MS Analysis

The mass spectral acquisition methods used in direct tissue analysis are performed in an automated fashion. When profiling discrete matrix spots, mass spectra are obtained by performing a raster over the area of interest on the tissue. The number of spectra obtained and averaged from a single spot on tissue depends on how many shots can be acquired at one location before the signal is depleted and how big the matrix spot is. Most experiments average between 250 and 500 spectra on a single spot about 150 μm in diameter. Mass spectral acquisition from spray-coated images does not involve averaging shots at different locations within a pixel. Instead, each ablated location
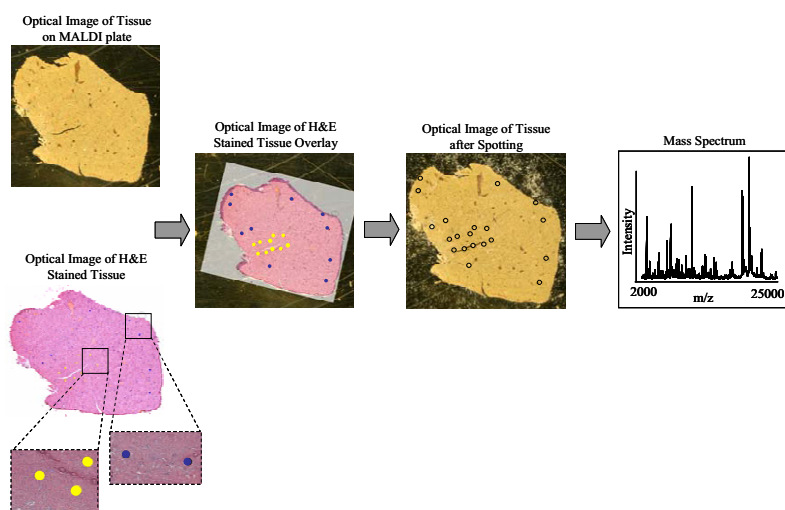

Figure 3. Histology-directed MS sample preparation for tissue analysis. A pathologist systematically selects discrete cellular areas (spots) of interest on a stained tissue section. The coordinates of the spots are transferred to the robotic spotter for matrix deposition on a co-registered serial section with subsequent laser irradiation of these spots (outlined in black for visualization) to give mass spectra.

represents one pixel and the number of laser shots within that pixel depends on how many shots can be obtained before the signal significantly decreases.

Spectral preprocessing is performed on the acquired data to reduce interexperimental and intra-experimental variance. Such variations may be produced from the ionization process, background noise, and calibration offsets that result from biological or sample preparation differences. Mass spectra are processed by removing background noise, normalizing intensities, and performing a final mass calibration. The latter is used primarily for profiling experiments in which multiple sample groups are being compared, enhancing the efficacy of statistical algorithms to determine biological patterns and changes in these patterns. Imaging applications typically do not require the recalibration step, but background subtraction and normalization significantly enhance the image quality. Illustrations of these processes have been presented.[24]

Data Analysis

The large, complex data sets produced by these experiments require robust bioinformatics tools to assess spectral patterns and to decipher molecular species that differentiate one group of samples from another. MS data from each group are compared to determine spectral features (peaks) that are significantly different between the 2 subject groups. The experimental design and biostatistical methods used are critical to the success of such analyses. Many of the algorithms used to decipher the vast amount of proteomic information were used initially for genomic microarray experiments and have been adapted for proteomic data set analyses.[25-28]

Protein Identification

Identification of statistically relevant mass spectral peaks is necessary to gain insight into biological processes. There are 2 approaches to protein identification. The top-down approach involves ionization and gas-phase fragmentation of the protein of interest inside the mass spectrometer,[29] whereas the bottom-up approach uses MS to identify peptides obtained from protease digestion of that protein, often in a mix-

ture of other proteolytic fragments.[30] The resulting mass spectra are searched against theoretical protein/peptide databases for corresponding sequence patterns. Searches are performed using conventional algorithms such as MASCOT and Sequest.[31,32] When possible, manual validation of reported identifications is recommended to reduce false-positive results.

Commonly, the bottom-up strategy is used and this involves homogenization of the tissue followed by reverse-phase liquid chromatography (RP-LC) separation, where the eluate continuously is collected into fractions. Fractions are vacuumed to dryness, dissolved in 40% acetonitrile with 0.1% TFA, spotted onto a MALDI plate, and analyzed for the fractions containing the peptides of interest. Based on the complexity of the fraction, one enzymatically can digest the entire fraction or further separate the mixture by 1-dimensional gel electrophoresis followed by excision and enzymatic digestion of the band of interest. Peptides then are subjected to further separation and fragmentation by RP-LC–tandem MS analysis and subsequent database searches.

On-tissue Digestion and Protein Identification

Recent work has shown that digestion and identification of proteins may be coupled with direct tissue analysis.[22] The technique involves automatically depositing a spotted array of enzymatic solution onto the tissue at room temperature. After hydrolysis, MALDI matrix (25 mg/mL 2,5-dihydroxybenzoic acid in 50% methanol, 0.5% TFA) is deposited onto the array for subsequent MALDI MS analysis. Figure 4 illustrates an image obtained from on-tissue tryptic digestion of a clear cell renal cell carcinoma (ccRCC) section, where a unique distribution of peptides is found in the tumor. This procedure provides the ability to simultaneously assess the distribution of proteins and their corresponding peptides by imaging MS (IMS) to obtain a more complete molecular signature of a tissue section. In addition, the in situ identification of proteins requires less time than conventional protein identification strategies and the ability to compare a given protein image to the image
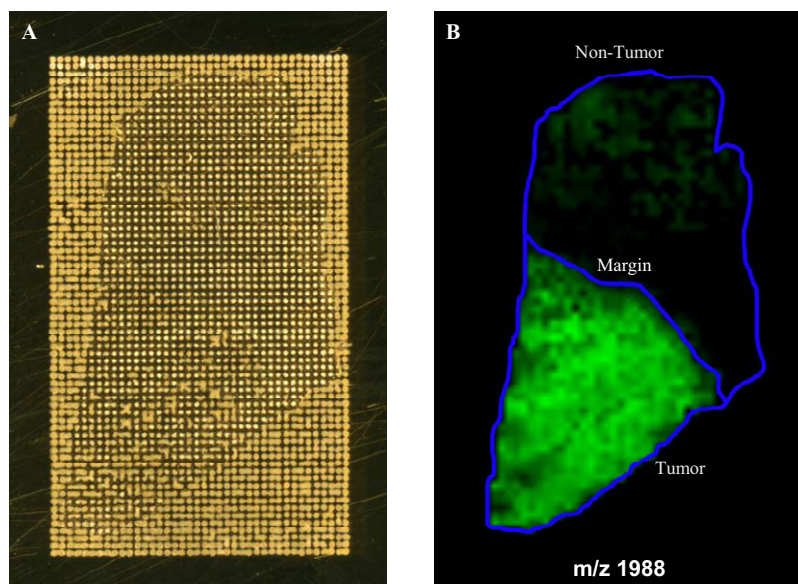
Figure 4. On-tissue tryptic digestion. Kidney tissue containing ccRCC and adjacent nontumor was sectioned at 12 μm thickness and transferred to a MALDI target plate. The section was washed with ethanol and spotted with an ordered array of 120 picoliter droplets of trypsin solution placed at 250 μm lateral resolution using a robotic spotter. Subsequent to hydrolysis, matrix (CHCA) was deposited directly on these spots and a peptide image was obtained. (A) Optical image of spotted trypsin and matrix array. (B) MALDI ion image of tryptic peptide m/z 1,988 localized to the tumor. Figure generated by M. Reid Groseclose.

of its subsequent peptides increases identification confidence. This process is best used for validation (ie, where the presence of one or more specific proteins is needed to be established). For unknown proteins, the bottom-up or top-down procedure is recommended.

Application to Kidney

Glomerulosclerosis

Focal segmental glomerulosclerosis (FSGS), or scarring of the glomeruli, is found in scattered regions of the kidney and impairs kidney function. Its etiology and biological causes are unknown, making treatment complicated and diagnosis difficult without a biopsy examination.[33] The focal segmental characteristic of FSGS provokes the question of whether the nonsclerotic glomeruli in sclerotic tissue already are programmed to become sclerotic or whether these nonsclerotic glomeruli have less prosclerotic activation and therefore are more receptive to therapy. By using direct tissue analysis by MALDI MS, Xu et al[34] used a glomerulosclerotic rat model to determine if proteomic profiles from sclerotic glomeruli could be differentiated

from nonsclerotic glomeruli, and, second, if nonsclerotic glomeruli have a prosclerotic phenotype at the protein level.

To achieve the selective isolation and analysis of glomeruli from tissue, laser capture microdissection (LCM) was used. This technique allows for the dissection of specific cells or cell populations from a heterogeneous tissue section. In the FSGS study, LCM was combined with MALDI MS for tissue protein profiling (Fig. 5). The LCM procedure requires that a thin tissue section (~8 μm thick) is mounted on a glass microscope slide and dehydrated in serial ethanol dilutions followed by xylene rinses. The LCM procedure uses a narrow laser beam (diameter, ~7-30 μm) to irradiate a heat-sensitive transparent polymer film, resulting in adhesion of the film to the section. The cells bound to the polymer are separated from the section when the polymer is removed. This polymer membrane is mounted onto a MALDI target plate using conductive double-sided tape. The cells are spotted with very small volumes of matrix (sinapinic acid) using a thin pulled capillary or a robotic matrix deposition device.
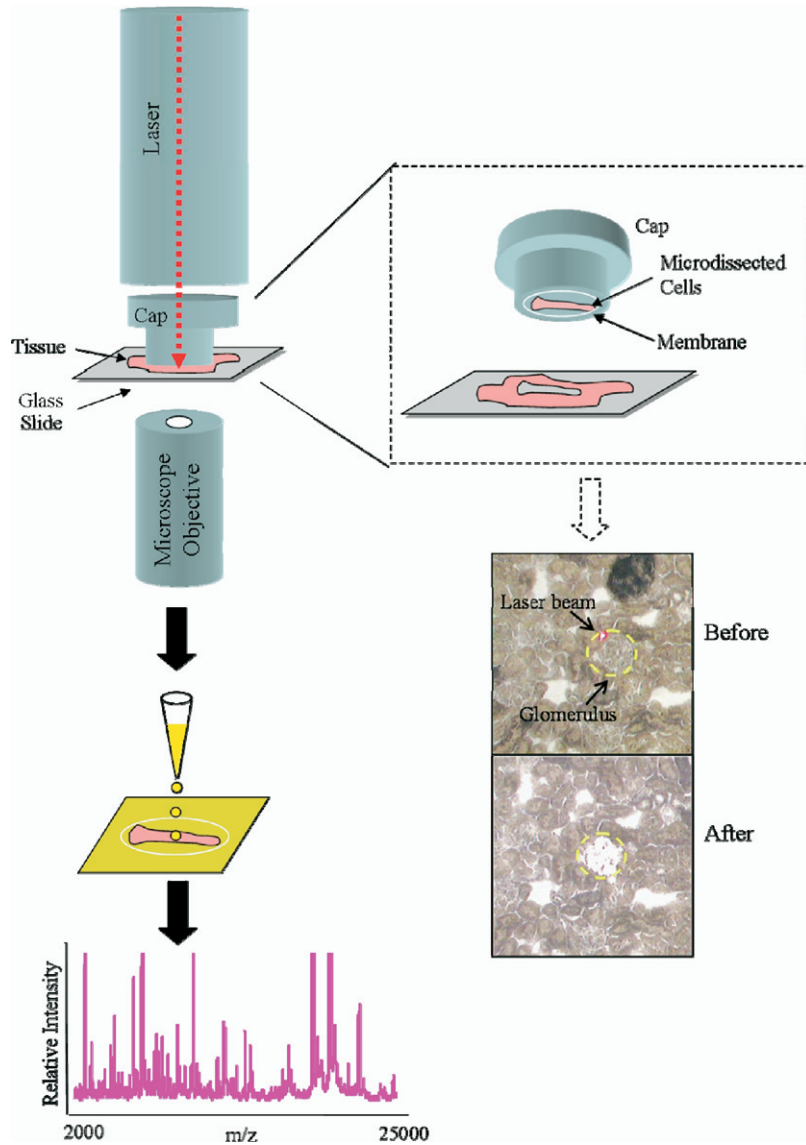
Figure 5. LCM preparation for MALDI MS analysis. A thin tissue section is placed on a glass slide where it is irradiated with a laser beam through a thermoplastic polymer film cap. When the cap is removed, cells that were irradiated remain attached to the cap. The cap is affixed to a MALDI plate and matrix is applied for subsequent MS analysis.

The analysis of LCM-captured cells combined with MALDI MS profiling and statistical analysis resulted in the proteomic differentiation and classification of normal, nonsclerotic, and sclerotic glomeruli. Statistical analysis revealed that nonsclerotic glomeruli in the presence of progressive renal scarring also have an altered proteomic profile that is more similar to sclerotic than normal glomeruli. For example, thymosin $\beta4$ was identified as one of several key differentiators between nonsclerotic and sclerotic glomeruli. Its expression also was increased in these samples as compared with normal glomeruli, suggesting its role as an early activator and indicator of prosclerotic mechanisms.

Drug Nephrotoxicity

The kidney is particularly susceptible to toxic damage because of its large surface area and its role in blood filtration. Current methods of assessing nephrotoxicity, such as monitoring serum creatinine levels and changes in cellular morphology, often fail to detect changes until the onset of toxic nephropathy. Characterization of toxicity markers with profiling and im-
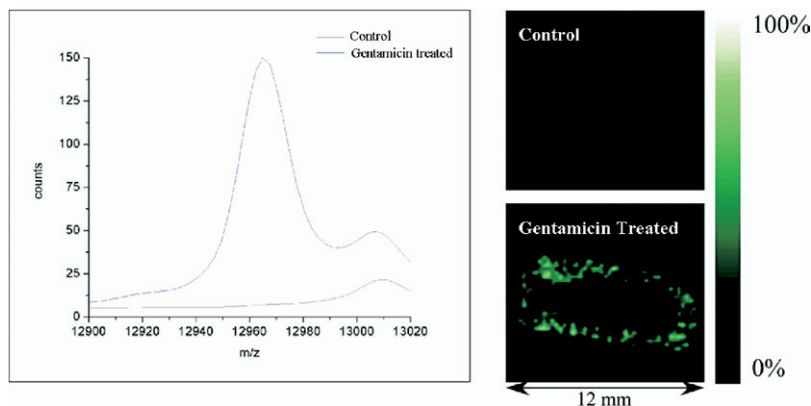
Figure 6. Imaging results from gentamicin study. Rats were dosed with gentamicin once daily for 7 days, killed, and their kidneys excised. Differential protein expression was compared between control and dosed kidneys using IMS. This figure shows the image analysis of m/z 12,959 differentially expressed in the cortex of dosed tissue with corresponding average peaks in the spectrum. Adapted with permission.[35]

aging MALDI MS may provide a robust and high-throughput method to detect toxicity in early lead compounds.

A pilot study was performed to examine the proteomic changes induced by gentamicin (Sigma, St. Louis, MO), an antibiotic known to cause proximal tubule damage in kidneys. Experimental details for this study have been described.[35] Briefly, male Wistar rats were treated for 7 consecutive days with 100 mg/kg/d gentamicin or vehicle and killed 24 hours after the last treatment. Kidney sections either were manually spotted for profiling or automatically spotted with an acoustic robotic spotter for imaging. Mass spectra from each region contained hundreds of peaks in the m/z range of 3,500 to 25,000. Some signals were confined to anatomic regions, such as the cortex, medulla, and papilla, giving each region its own molecular signature. Notably, a peak at m/z 12,959 was found to be statistically significant in differentiating control and treated animals. IMS results indicated that this feature was localized to the cortex, the site of damage in these animals (Fig. 6). This protein was extracted directly from the cortex of 3 tissue sections and the extracts were pooled and separated by RP-LC. The LC fraction containing the peak of interest was subjected to RP-LC–tandem MS analysis and identified as transthyretin, a marker of nutritional status[36-38] and a ligand of the megalin receptor,[39] which binds gentamicin.[40,41] The identification was confirmed by Western blot and immunohistochemistry.

Renal Tumor Margins

Another study currently ongoing is the investigation of the molecular distributions in ccRCC with respect to molecular tumor margins. One of the major concerns in clinical oncology is ensuring complete tumor removal to minimize local recurrence and ensure long-term patient survival.[42-44] Depending on the tumor type, recurrence can occur a few months to a few years after removal of the primary tumor, suggesting that there are underlying molecular processes in the remaining normal tissue that go undetected using current histopathologic techniques. The discovery of new molecular markers for these processes has the potential to provide additional complementary approaches to identify abnormal tissue environments.

It is important to be able to measure the molecular characteristics of the tumor and surrounding tumor margin of ccRCC. The radical nephrectomy procedure is the standard treatment for ccRCC, but it is excessive for small tumors or patients in whom the tumor is confined to a solitary functioning kidney, has arisen bilaterally, or when the remaining kidney could be under future threat from renal deficiencies. The partial nephrectomy procedure maximizes the amount of kidney spared but presents a challenge for clinicians because of concerns over tumor involvement of the surgical margin.[45-47]
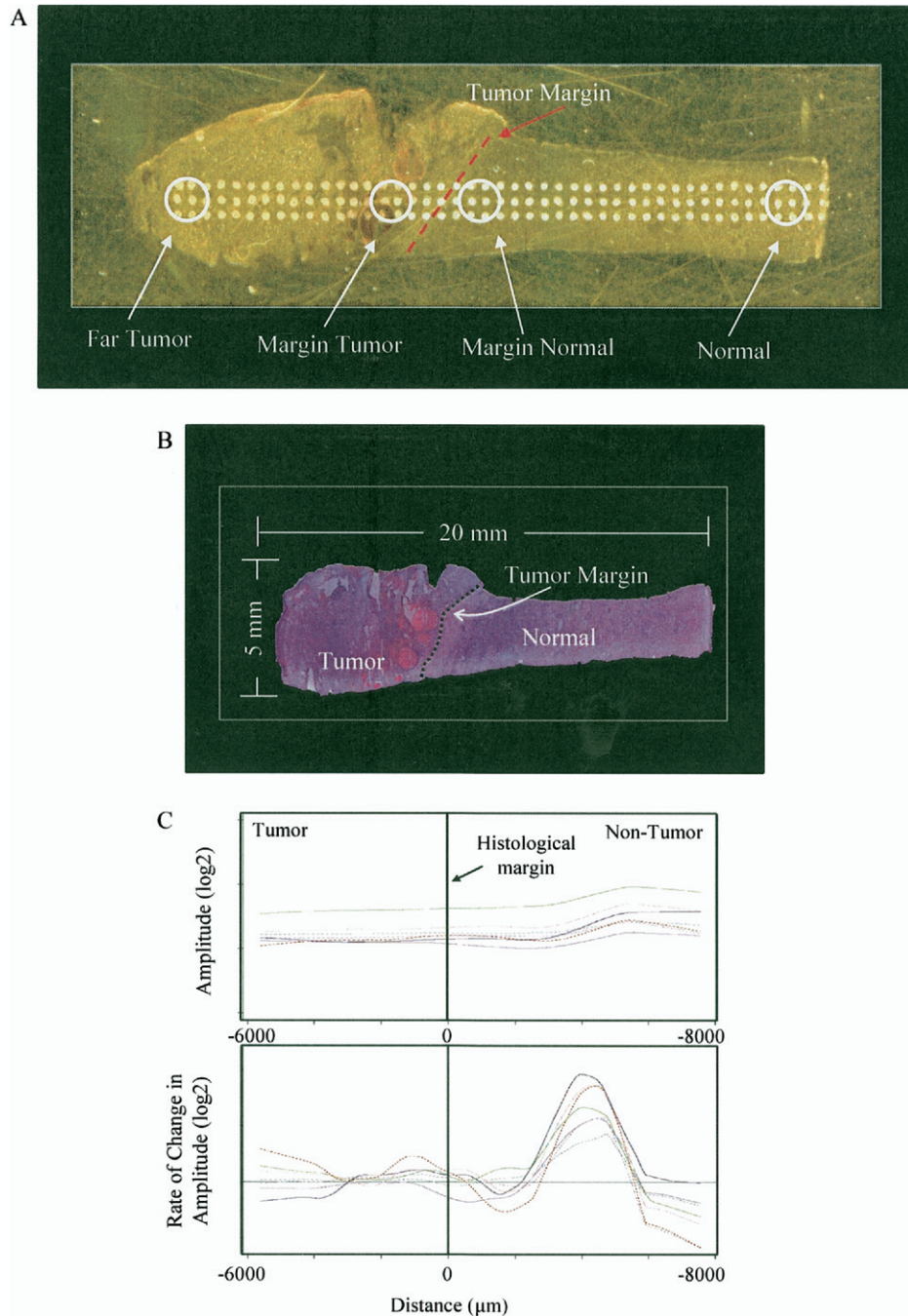
Figure 7. Tumor margin analysis by MALDI MS. (A) Optical image of section with matrix spots with regions of interest highlighted. (B) Optical image of the corresponding hematoxylin-eosin–stained section. (C) The top figure shows the amplitude of 6 m/z values plotted as a function of distance (of corresponding matrix spot analyzed) from the histologic tumor margin in one representative tissue sample. Each line represents a different m/z value, each identified as a member of the mitochondrial electron transport chain. These are smoothed trend lines of the original scatterplot data. The bottom figure is a plot of the first derivative of the trend line. Both plots illustrate that the features represented are underexpressed in the tumor and in the margin normal tissue. These features remain underexpressed until approximately 4,000 μm past the histologic tumor border.

Proteomic technologies such as profiling/ imaging MALDI MS may allow for the elucidation of tumor margin characteristics to further understand tumor spread. Early results have identified molecular signatures that show atypical tissue significantly beyond the histologic margin. MALDI-TOF MS was performed on 34 ccRCC biopsy specimens containing tumor and adjacent nontumor tissue. Matrix arrays were deposited on the tissue, covering the tumor and nontumor tissue (Fig. 7A). Automated MS acquisition was performed on each of the matrix spots. After processing mass spectra, statistical analysis was performed on the regions as follows: tumor versus normal and margin normal versus normal (Fig. 7B). Many of the differences between tissue on the normal side of the margin and tissue distant normal also were observed between tumor and nearby histologically normal tissue. Protein identification revealed that one of the families contributing to these abnormal characteristics was mitochondrial electron transport proteins. These proteins were underexpressed in the tumor as compared with normal and underexpressed in the near-normal compared with normal (Fig. 6C). Based on the results as well as other studies,[48-56] it is probable that increased glycolysis at the expense of mitochondrial oxidative phosphorylation plays a significant role in ccRCC tumor spread into the normal tissue.

CONCLUSIONS

Direct tissue analysis by MALDI MS is an important technology for assessing the localization of molecular species and for revealing the underlying molecular signatures indicative of disease. The molecular species identified in these experiments can provide insight into mechanisms and etiology of disease. Applications to kidney diseases have just begun, but the potential of this technology to help unravel the complex molecular processes involved are extraordinary. With increasing advances in the field, the utility of this technology will continue to evolve and will play a fundamental role in understanding kidney biology.

REFERENCES

1. Hillenkamp F, Karas M, Beavis RC, Chait BT. Matrix-assisted laser desorption/ionization mass spectrometry of biopolymers. Anal Chem. 1991;63:1193A-203A.
2. Karas M, Hillenkamp F. Laser desorption ionization of proteins with molecular masses exceeding 10,000 daltons. Anal Chem. 1988;60:2299-301.
3. Chaurand P, Caprioli RM. Direct profiling and imaging of peptides and proteins from mammalian cells and tissue sections by mass spectrometry. Electrophoresis. 2002;23:3125-35.
4. Schwartz SA, Reyzer ML, Caprioli RM. Direct tissue analysis using matrix-assisted laser desorption/ionization mass spectrometry: practical aspects of sample preparation. J Mass Spectrom. 2003;38:699-708.
5. Caprioli RM, Farmer TB, Gile J. Molecular imaging of biological samples: localization of peptides and proteins using MALDI-TOF MS. Anal Chem. 1997;69:4751-60.
6. Karas M, Gluckmann M, Schafer J. Ionization in matrix-assisted laser desorption/ionization: singly charged molecular ions are the lucky survivors. J Mass Spectrom. 2000;35:1-12.
7. Zenobi R, Knochenmuss R. Ion formation in MALDI mass spectrometry. Mass Spectrom Rev. 1998;17:337-6.
8. Wiley WC, McLaren IH. Time-of-flight mass spectrometer with improved resolution. Rev Sci Instruments. 1955;26:1150-1157.
9. Cotter RJ. The new time-of-flight mass spectrometry. Anal Chem. 1999;71:445A-51A.
10. Khatib-Shahidi S, Andersson M, Herman JL, Gillespie TA, Caprioli RM. Direct molecular analysis of whole-body animal tissue sections by imaging MALDI mass spectrometry. Anal Chem. 2006;78:6448-56.
11. Reyzer ML, Caprioli RM. MALDI-MS-based imaging of small molecules and proteins in tissues. Curr Opin Chem Biol. 2007;11:29-35.
12. Troendle FJ, Reddick CD, Yost RA. Detection of pharmaceutical compounds in tissue by matrix-assisted laser desorption/ionization and laser desorption/ chemical ionization tandem mass spectrometry with a quadrapole ion trap. J Am Soc Mass Spectrom. 1999;10:1315-21.
13. Reyzer ML, Hsieh Y, Ng K, Korfmacher WA, Caprioli RM. Direct analysis of drug candidates in tissue by matrix-assisted laser desorption/ionization mass spectrometry. J Mass Spectrom. 2003;38:1081-92.
14. Stoeckli M, Chaurand P, Hallahan DE, Caprioli RM. Imaging mass spectrometry: a new technology for the analysis of protein expression in mammalian tissues. Nat Med. 2001;7:493-6.
15. Chaurand P, Cornett DS, Caprioli RM. Molecular imaging of thin mammalian tissue sections by mass spectrometry. Curr Opin Biotechnol. 2006;17:431-6.
16. Schwartz SA, Weil RJ, Johnson MD, Toms SA, Caprioli RM. Protein profiling in brain tumors using mass spectrometry: feasibility of a new technique for the analysis of protein expression. Clin Cancer Res. 2004;10:981-7.
17. Schwartz SA, Weil RJ, Thompson RC, Shyr Y, Moore JH, Toms SA, et al. Proteomic-based prognosis of brain

tumor patients using direct-tissue matrix-assisted laser desorption ionization mass spectrometry. Cancer Res. 2005;65:7674-81.

18. Srinivasan M, Sedmak D, Jewell S. Effect of fixatives and tissue processing on the content and integrity of nucleic acids. Am J Pathol. 2002;161:1961-71.

19. Aerni HR, Cornett DS, Caprioli RM. Automated acoustic matrix deposition for MALDI sample preparation. Anal Chem. 2006;78:827-34.

20. Xu BJ, Caprioli RM, Sanders ME, Jensen RA. Direct analysis of laser capture microdissected cells by MALDI mass spectrometry. J Am Soc Mass Spectrom. 2002;13:1292-7.

21. Cornett DS, Mobley JA, Dias EC, Andersson M, Arteaga CL, Sanders ME, et al. A novel histology-directed strategy for MALDI-MS tissue profiling that improves throughput and cellular specificity in human breast cancer. Mol Cell Proteomics. 2006;5:1975-83.

22. Groseclose MR, Andersson M, Hardesty WM, Caprioli RM. Identification of proteins directly from tissue: in situ tryptic digestions coupled with imaging mass spectrometry. J Mass Spectrom. 2007;42:254-62.

23. Chaurand P, Schwartz SA, Billheimer D, Xu BJ, Crecelius A, Caprioli RM. Integrating histology and imaging mass spectrometry. Anal Chem. 2004;76:1145-55.

24. Norris JL, Cornett DS, Mobley JA, Andersson M, Seeley EH, Chaurand P, et al. Processing MALDI mass spectra to aid biomarker discovery and improve mass spectral image quality. Int J Mass Spectrom. 2007;260:212-21.

25. Tusher VG, Tibshirani R, Chu G. Significance analysis of microarrays applied to the ionizing radiation response (vol 98, pg 5116, 2001). Proc Natl Acad Sci U S A. 2001;98:10515.

26. Naiman DQ. Random data set generation to support microarray analysis. Methods Enzymol. 2006;411:312-25.

27. Hedenfalk I, Duggan D, Chen Y, Radmacher M, Bittner M, Simon R, et al. Gene-expression profiles in hereditary breast cancer. N Engl J Med. 2001;344:539-48.

28. Storey JD, Tibshirani R. Statistical significance for genomewide studies. Proc Natl Acad Sci U S A. 2003;100:9440-5.

29. Reid GE, McLuckey SA. 'Top down' protein characterization via tandem mass spectrometry. J Mass Spectrom. 2002;37:663-75.

30. Wysocki VH, Resing KA, Zhang Q, Cheng G. Mass spectrometry of peptides and proteins. Methods. 2005;35:211-22.

31. Hirosawa M, Hoshida M, Ishikawa M, Toya T. MASCOT: multiple alignment system for protein sequences based on three-way dynamic programming. Comput Appl Biosci. 1993;9:161-7.

32. Link AJ, Eng J, Schieltz DM, Carmack E, Mize GJ, Morris DR, et al. Direct analysis of protein complexes using mass spectrometry. Nat Biotechnol. 1999;17:676-82.

33. Ponticelli C, Villa M, Banfi G, Cesana B, Pozzi C, Pani A, et al. Can prolonged treatment improve the prognosis in adults with focal segmental glomerulosclerosis? Am J Kidney Dis. 1999;34:618-25.

34. Xu BJ, Shyr Y, Liang X, Ma LJ, Donnert EM, Roberts JD, et al. Proteomic patterns and prediction of glomerulosclerosis and its mechanisms. J Am Soc Nephrol. 2005;16:2967-75.

35. Meistermann H, Norris JL, Aerni HR, Cornett DS, Friedlein A, Erskine AR, et al. Biomarker discovery by imaging mass spectrometry: transthyretin is a biomarker for gentamicin-induced nephrotoxicity in rat. Mol Cell Proteomics. 2006;5:1876-86.

36. Bernstein LH, Ingenbleek Y. Transthyretin: its response to malnutrition and stress injury. Clinical usefulness and economic implications. Clin Chem Lab Med. 2002;40:1344-8.

37. Ingenbleek Y, Young V. Transthyretin (prealbumin) in health and disease: nutritional implications. Annu Rev Nutr. 1994;14:495-533.

38. Lasztity N, Biro L, Nemeth E, Pap A, Antal M. Protein status in pancreatitis—transthyretin is a sensitive biomarker of malnutrition in acute and chronic pancreatitis. Clin Chem Lab Med. 2002;40:1320-4.

39. Sousa MM, Norden AG, Jacobsen C, Willnow TE, Christensen EI, Thakker RV, et al. Evidence for the role of megalin in renal uptake of transthyretin. J Biol Chem. 2000;275:38176-81.

40. Verroust PJ, Birn H, Nielsen R, Kozyraki R, Christensen EI. The tandem endocytic receptors megalin and cubilin are important proteins in renal pathology. Kidney Int. 2002;62:745-56.

41. Moestrup SK, Cui S, Vorum H, Bregengard C, Bjorn SE, Norris K, et al. Evidence that epithelial glycoprotein 330/megalin mediates uptake of polybasic drugs. J Clin Invest. 1995;96:1404-13.

42. Balch GC, Mithani SK, Simpson JF, Kelley MC. Accuracy of intraoperative gross examination of surgical margin status in women undergoing partial mastectomy for breast malignancy. Am Surg. 2005;71:22-8.

43. Looser KG, Shah JP, Strong EW. The significance of "positive" margins in surgically resected epidermoid carcinomas. Head Neck Surg. 1978;1:107-11.

44. Nathan CO, Amirghahri N, Rice C, Abreo FW, Shi R, Stucker FJ. Molecular analysis of surgical margins in head and neck squamous cell carcinoma patients. Laryngoscope. 2002;112:2129-40.

45. Dechet CB, Zincke H, Sebo TJ, King BF, LeRoy AJ, Farrow GM, et al. Prospective analysis of computerized tomography and needle biopsy with permanent sectioning to determine the nature of solid renal masses in adults. J Urol. 2003;169:71-4.

46. Nguyen TT, Parkinson JP, Kuehn DM, Winfield HN. Technique for ensuring negative surgical margins during laparoscopic partial nephrectomy. J Endourol. 2005;19:410-5.

47. Sengupta S, Zincke H. Lessons learned in the surgical management of renal cell carcinoma. Urology. 2005;66:36-42.

48. Acker T, Fandrey J, Acker H. The good, the bad and the ugly in oxygen-sensing: ROS, cytochromes and prolylhydroxylases. Cardiovasc Res. 2006;71:195-207.

49. Gatenby RA, Gawlinski ET. The glycolytic phenotype in carcinogenesis and tumor invasion: insights through mathematical models. Cancer Res. 2003;63:3847-54.

50. Giaccia AJ, Simon MC, Johnson R. The biology of hypoxia: the role of oxygen sensing in development, normal function, and disease. Genes Dev. 2004;18: 2183-94.

51. Guzy RD, Schumacker PT. Oxygen sensing by mitochondria at complex III: the paradox of increased reactive oxygen species during hypoxia. Exp Physiol. 2006;91:807-19.

52. Haase VH. The VHL/HIF oxygen-sensing pathway and its relevance to kidney disease. Kidney Int. 2006;69: 1302-7.

53. Hervouet E, Demont J, Pecina P, Vojtiskova A, Houstek J, Simonnet H, et al. A new role for the von Hippel-Lindau tumor suppressor protein: stimulation of mitochondrial oxidative phosphorylation complex biogenesis. Carcinogenesis. 2005;26:531-9.

54. Raghunand N, Gatenby RA, Gillies RJ. Microenvironmental and cellular consequences of altered blood flow in tumours. Br J Radiol. 2003;76:S11-22.

55. Simonnet H, Alazard N, Pfeiffer K, Gallou C, Beroud C, Demont J, et al. Low mitochondrial respiratory chain content correlates with tumor aggressiveness in renal cell carcinoma. Carcinogenesis. 2002;23:759-68.

56. Warburg O. The metabolism of tumors. London: Constable Press; 1930.